Acta Neuropathol (2017) 133:381–393
DOI 10.1007/s00401-016-1661-y

ORIGINAL PAPER

Brain-to-stomach transfer of α-synuclein via vagal preganglionic projections

Ayse Ulusoy[1] · Robert J. Phillips[2] · Michael Helwig[1] · Michael Klinkenberg[1] · Terry L. Powley[2] · Donato A. Di Monte[1]

Received: 27 October 2016 / Revised: 16 December 2016 / Accepted: 16 December 2016 / Published online: 23 December 2016

Abstract Detection of α-synuclein lesions in peripheral tissues is a feature of human synucleinopathies of likely pathogenetic relevance and bearing important clinical implications. Experiments were carried out to elucidate the relationship between α-synuclein accumulation in the brain and in peripheral organs, and to identify potential pathways involved in long-distance protein transfer. Results of this in vivo study revealed a route-specific transmission of α-synuclein from the rat brain to the stomach. Following targeted midbrain overexpression of human α-synuclein, the exogenous protein was capable of reaching the gastric wall where it was accumulated into preganglionic vagal terminals. This brain-to-stomach connection likely involved intra- and inter-neuronal transfer of non-fibrillar α-synuclein that first reached the medulla oblongata, then gained access into cholinergic neurons of the dorsal motor nucleus of the vagus nerve and finally traveled via efferent fibers of these neurons contained within the vagus nerve. Data also showed a particular propensity of vagal motor neurons and efferents to accrue α-synuclein and deliver it to peripheral tissues; indeed, following its midbrain overexpression, human α-synuclein was detected within gastric nerve endings of visceromotor but not viscerosensory vagal projections. Thus, the dorsal motor nucleus of the vagus nerve represents a key relay center for central-to-peripheral α-synuclein transmission, and efferent vagal fibers may act as unique conduits for protein transfer. The presence of α-synuclein in peripheral tissues could reflect, at least in some synucleinopathy patients, an ongoing pathological process that originates within the brain and, from there, reaches distant organs innervated by motor vagal projections.

Keywords Adeno-associated virus · Enteric nervous system · Parkinson's disease · Rat · Synucleinopathies · Vagus nerve

Introduction

Intraneuronal inclusions containing α-synuclein are hallmarks of Parkinson's disease and other neurological disorders such as dementia with Lewy bodies and multiple system atrophy [11, 22]. In typical Parkinson's disease, α-synuclein pathology is characterized by a progressive caudo-rostral advancement; initial lesions are observed in the lower brainstem and, in particular, the dorsal motor nucleus of the vagus nerve (DMnX) from where α-synuclein pathology spreads toward mesencephalic and ultimately cortical brain regions [6]. An important role of the DMnX and vagal connections in Parkinson's disease pathogenesis is further suggested by findings showing accumulation of α-synuclein deposits in the gut; this accumulation followed a pattern that matched the distribution of preganglionic terminals of DMnX-derived vagal efferents [2]. It has been hypothesized that the pathological process of Parkinson's disease, perhaps mediated by toxic α-synuclein species, may proceed from distant nerve endings in the gut toward the brain or, vice versa, from the

Electronic supplementary material The online version of this article (doi:10.1007/s00401-016-1661-y) contains supplementary material, which is available to authorized users.

✉ Donato A. Di Monte
donato.dimonte@dzne.de

[1] German Center for Neurodegenerative Diseases (DZNE), Sigmund-Freud-Strasse 27, 53127 Bonn, Germany

[2] Department of Psychological Sciences, Purdue University, 703 Third Street, West Lafayette, IN 47907-2081, USA

DMnX to the enteric nervous system following the course of the vagus nerve [11]. It has also been proposed that long, unmyelinated axons, such as those originating from DMnX neurons, may be particularly vulnerable to α-synuclein transfer and its pathological accumulation [6].

Several experimental studies in animal models support the ability of α-synuclein to move efficiently throughout the brain via intra- and inter-neuronal protein transmission [9, 23]. Some of these investigations have shown that α-synuclein can advance caudo-rostrally from the gastrointestinal tract to the brain and from lower to higher brain regions [12, 13, 15, 25]. No direct evidence to date, however, supports the ability of α-synuclein to travel long-distance in the opposite direction, from the brain parenchyma to peripheral nerve endings. Similarly, the hypothesis that distinct neuronal populations and, in particular, visceromotor vagal neurons, may contribute to a greater degree to the progression of α-synuclein pathology remains unsubstantiated from the experimental standpoint. Results of the present study provide important new clues on the central-to-peripheral and route-specific transmission of α-synuclein. Data reveal that viral vector-mediated overexpression of human α-synuclein (hα-synuclein) in the rat midbrain triggers its advancement via the vagus nerve and results in its pathological accumulation in the stomach wall. Interestingly, this accumulation targeted preganglionic vagal terminals while it did not occur within viscerosensory gastric afferents, pointing to a preferential route of protein transmission via neurons, namely DMnX cells and their projections, that are particularly able to accrue and deliver α-synuclein.

Materials and methods

Viral vectors

Recombinant adeno-associated viral vectors (AAVs; serotype 2 genome and serotype 6 capsid) were used for transgene expression of hα-synuclein or green fluorescent protein (GFP; Vector Biolabs). Expression, driven by the human *SYN1* promoter, was enhanced using woodchuck hepatitis virus post-transcriptional regulatory element (WPRE) and a polyadenylation signal sequence.

Animals and surgical procedure

Experimental procedures involving animals were approved by the State Agency for Nature, Environment and Consumer Protection in North Rhine Westphalia. Experiments were performed in female Sprague-Dawley rats (200–225 g; Charles River) housed under a 12-h light/12-h dark cycle with free access to food and water. During surgical procedures, rats were anesthetized with 2% isoflurane mixed with O_2 and N_2O. Each animal received a single unilateral injection of AAV solution (1.0×10^{13} genome copies/ml) either (1) into the left vagus nerve in the neck (2 µl), or (2) intraparenchymally, into the right ventral mesencephalon immediately dorsal to the substantia nigra pars compacta (1 µl). Vagal injections were made according to previously described protocols [25]. To target the substantia nigra, the following stereotaxic coordinates were used with a tooth bar setting of −2.3: 5.0 mm posterior and 2.0 mm lateral to bregma, and 7.1 mm ventral to dura mater. The injection was made at a rate of 0.4 µl/min using a Hamilton syringe fitted to a glass capillary. The capillary was left in position for 5 min before being withdrawn.

Tissue preparation

Animals were killed with pentobarbital. Brains used for in situ hybridization were snap frozen on dry ice and stored at −80 °C. At the time of analysis, they were cryosectioned (14 µm) and then mounted on polysine object slides. For histological analyses, rats were perfused through the ascending aorta first with physiological saline solution. At this time, a cannula was inserted via oral gavage to inflate the stomach with 10 ml saline. The perfusion continued using 4% ice-cold paraformaldehyde in 0.1 M phosphate buffer. The following organs/tissues were collected: brain, vagus nerve (including the nodose ganglion) in the rat neck and stomach. Brains and vagus nerves were post-fixed in 4% paraformaldehyde solution for 24 h and cryopreserved in 25% (w/v) sucrose solution. Coronal sections (40 µm) throughout the brain were cut using a freezing microtome, while each vagus nerve was sectioned (16 µm) longitudinally using a cryostat. Stomachs were post-fixed but not cryopreserved. They were divided into dorsal and ventral whole mounts by cutting along the greater and lesser curvatures.

Assays

All analyses, as described in the next paragraphs, were performed by investigators blinded to treatment/experimental group.

Brightfield microscopy

Medulla oblongata

Free-floating sections were quenched by incubations in a mixture of 3% H_2O_2 and 10% methanol in Tris-buffered saline (pH 7.6). Non-specific binding sites were blocked by incubations in Tris-buffered saline with 0.25% Triton X-100 containing 5% normal serum. Samples were

kept overnight at room temperature in a solution (Tris-buffered saline with 1% BSA and 0.25% Triton X-100) containing the primary antibody, i.e., mouse anti-hα-synuclein clone syn211 (36-008, Merck Millipore; 1:10 000). Sections were rinsed and incubated (for 1 h at room temperature) in biotinylated secondary antibody solution (Vector Laboratories; 1:200). Following treatment with avidin-biotin-horseradish peroxidase complex (PK 6100; ABC Elite kit, Vector Laboratories), color reaction was developed using a 3,3′-diaminobenzidine (DAB) kit (Vector Laboratories). Sections were mounted on coated slides, dried and coverslipped with Depex (Sigma-Aldrich). Stacked or tiled images collected with 40× or 10× Plan-Apochromat, respectively, were obtained using an IX2 UCB microscope from Olympus equipped with a motorized stage and camera (MBF Biosciences). Stacks were collected at 1 µm intervals, and a single image was generated by deep focus post-processing using Stereo Investigator software (version 9, MBF Biosciences). In a set of analyses, the percent of DMnX neurons overexpressing hα-synuclein was calculated after hα-synuclein-AAV injections into the rat vagus nerve. For these analyses, both the total number of Nissl-stained cells and the number of hα-synuclein-positive neurons was estimated using unbiased stereology [24].

Vagus nerve and nodose ganglion

Sections on slides were quenched and blocked as described above. They were incubated for 48 h at 4 °C in mouse anti-hα-synuclein (syn211; 1:2000) or chicken anti-GFP (ab13970, Abcam; 1:5000) and for 1 h at room temperature in ImmPRESS secondary antibody (Vector Laboratories). Color reaction was developed using a DAB kit. Images were collected using an Axiocam 503 color camera fitted to an Axioscope microscope (Zeiss).

Stomach

The mucosa and submucosa were removed by fine dissection, and the resulting smooth muscle whole mounts were rinsed in PBS followed by a 30-min soak in an endogenous peroxidase block (methanol:3% H_2O_2; 4:1). After additional rinses in PBS, the neuronal population of the myenteric plexus was counterstained with the pan-neuronal marker Cuprolinic Blue (quinolinic phthalocyanine; Polysciences). Whole mounts were then soaked for 5 days in normal serum block (0.5% Triton X-100, 5% normal serum, 2% BSA, and 0.08% Na Azide in PBS) followed by a 24 h soak in antiserum raised against hα-synuclein (syn211; 1:5000) or GFP (ab13970; 1:10 000) in primary diluent (0.3% Triton X-100, 2% normal serum, 2% BSA, and 0.08% Na Azide in PBS). Next, whole mounts were rinsed in PBS and incubated for 2 h in diluent (0.3% Triton X-100, 2% normal serum, and 2% BSA in PBS) with appropriate biotinylated secondary antibody (Vector Laboratories; 1:500). After several more PBS rinses, tissues were incubated for 1 h in avidin-biotin-horseradish peroxidase complex (Vector Laboratories) in PBS. Horseradish peroxidase was reacted with DAB and H_2O_2 in Tris-buffered saline for 3 min to yield a permanent deposit. Finally, stained whole mounts were mounted on gelatin-coated slides, air-dried overnight, dehydrated in an ascending series of alcohols, cleared in two xylene steps, and coverslipped with Cytoseal XYL (Richard-Allen Scientific). Brightfield photomicrographs were acquired using a Leica microscope fitted with a Spot Flex camera that was controlled using Spot Software (V4.7 Advanced Plus; Diagnostic Instruments).

Fluorescent microscopy

Free-floating sections were blocked in 5% horse serum and incubated in 1% BSA with the following primary antibodies raised against: hα-synuclein (syn211; 1:3000), GFP (ab13970; 1:5000), choline acetyltransferase (ChAT) (AB144, Merck Millipore; 1:100), Syn-O2 (1:2000) or Syn-F1 (1:1000). The latter two antibodies, gifts from Dr. O. El-Agnaf, have been previously characterized [26]. Appropriate fluorophore-conjugated secondary antibodies (DyLight 488 and DyLight 594, from Vector Laboratories; Alexa 488 and Alexa 594, from Abcam) (1:400) were used for detection, and samples were mounted and coverslipped using Vectashield mounting medium (Vector Laboratories). Sequential scans were performed with 10× and 63× Plan-Apochromat objectives using either (1) a LSM710NLO confocal laser scanning microscope (Carl Zeiss) with tunable lasers set at 490 and 595 nm, or (2) an IX2 UCB microscope (Olympus) with a DSU spinning disk unit (Olympus), a motorized stage (MBF Biosciences) and an EM-CCD camera (Hamamatsu). As negative controls, tissue sections were processed as described above with the only exception that the primary antibody (e.g., anti-ChAT) was omitted from the initial incubations (Supplementary Figure 1).

Fluorescent in situ hybridization

Samples were processed following a protocol modified from Raj et al. [19]. Twenty-six individual probes (18 bp each) were designed against WPRE and generated with 3′-amino modifications (BioSearch Technologies) coupled to a Quasar 570 fluorophore. Sections were first equilibrated to room temperature, fixed with 4% paraformaldehyde, washed with PBS and stored overnight in 70% ethanol. On the next day, after washing, they were incubated overnight at 37 °C in hybridization buffer containing labeled probes (125 nM) and, when needed, primary

antibodies. The following antibodies were used: anti-hα-synuclein (syn211; 1:1000) and anti-ChAT (AB144; 1:100). After washing, sections for in situ hybridization/immunofluorescence were incubated for 2 h at room temperature in PBS with DyLight 488 and DyLight 649 secondary antibodies (Vector Laboratories; 1:200). Samples were labeled with 4′,6-diamidino-2-phenylindole (5 ng/ml), washed and finally mounted with Vectashield mounting medium (Vector Laboratories). Images were obtained using a Zeiss Observer.Z1 Microscope (Carl Zeiss) equipped with a motorized stage and AxioCam MRm camera (Carl Zeiss). Figures were generated with 20× Plan-Apochromat (NA 0.8) and 63× Plan-Apochomat (NA 1.4) objectives followed by computerized image stitching with ZEN 2 software (Carl Zeiss).

RT-PCR

Samples were obtained from 40-µm fixed tissue sections. The right (injection side) ventral mesencephalon or dorsomedial portion of the medulla oblongata were dissected and pooled from equally spaced sections at Bregma: −4.56 to −6.48 mm or Bregma: −13.68 to −14.64 mm. RNA was extracted using Nucleic Acid Isolation Kit (Ambion). cDNA was synthesized using 100 ng of total RNA (SuperScript® VILO Master Mix, Life Technologies). cDNA was amplified (30 cycles) using Power SYBR® Green (Applied Biosystems) and 0.25 µM primers (Sigma-Aldrich) in a StepOnePlus Real-Time PCR System (Applied Biosystems). Primer pairs matching DNA sequences were: (1) 5′caattccgtggtgttgtcgg forward and 5′caaagggagatccgactcgt reverse (WPRE); (2) 5′aatgaagaaggagccccacag forward and 5′aaggcatttcataagcctcattgtc reverse (hα-synuclein); (3) 5′acgacggcaactacaagacc forward and 5′tcctccttgaagtcgatgcc reverse (GFP); (4) 5′gaccggttctgtcatgtcg forward and 5′acctggttcatcatcactaatcac reverse (hypoxanthine phosphoribosyltransferase 1). RT-PCR products were separated on agarose gels. DNA signals were visualized with Gel Red Nucleic Acid Gel Stain (Biotium) and imaged with InGenius imaging system and GeneSnap software (Syngene).

Results

Efferent and afferent vagal terminals in the gastric wall

The first set of experiments was designed to assess the distribution of hα-synuclein and its accumulation within gastric nerve endings following its overexpression directly in the vagal system. AAVs carrying the DNA for hα-synuclein or GFP were injected into the left vagus nerve in the rat neck with the intent of transducing DMnX cells in the medulla oblongata as well as neuronal cell bodies within vagal ganglia, in particular the nodose ganglion (Fig. 1a, c). In agreement with previously published results [24], approximately 30% of the total DMnX neurons showed robust overexpression of hα-synuclein after vagal injections of hα-synuclein-AAVs (Fig. 1b). Accumulation of the exogenous protein within gastric nerve endings was then assessed in animals killed several months (>6 months) after AAV treatment. Stomach whole mounts consisting of the longitudinal and circular smooth muscle layers encompassing the myenteric plexus were stained with a specific antibody that recognizes human but not rodent α-synuclein [10]. Robust immunoreactivity characterized fibers and nerve endings that, because of their morphology, could be identified as afferent vagal projections originating from neurons of the nodose ganglion [16, 28]. In particular, hα-synuclein was accumulated within intramuscular arrays (IMAs) of rectilinear terminals paralleling smooth muscle fibers and within highly arborizing intraganglionic laminar endings (IGLEs), the two main types of afferent vagal terminals (Fig. 1d, e). Earlier work has also elucidated the morphological features of efferent vagal fibers and nerve endings arising from cell bodies in the DMnX and terminating in the gastric wall [16, 27]. Immunoreactivity for hα-synuclein labeled preganglionic axons that, consistent with these features, formed varicosity-rich telodendria looping around a single neuron or multiple ganglionic cells (Fig. 1f). Similar to treatment with hα-synuclein-carrying AAVs, vagal injections of GFP-AAVs resulted in accumulation of the transduced protein within both viscerosensory and visceromotor projections in the rat stomach wall (data not shown).

Long-distance transmission of human α-synuclein from the brain to the stomach

To determine if α-synuclein was capable of traveling long-distance from the brain to peripheral tissues, hα-synuclein-carrying AAVs were unilaterally (right side) injected into the rat ventral mesencephalon immediately dorsal to the substantia nigra pars compacta. Animals were killed at 2, 6 or 12 months, and the distribution of hα-synuclein throughout the brain was evaluated in tissue sections rostral and caudal to the midbrain. Immunoreactivity for hα-synuclein was observed in sections spanning from the forebrain to the medulla oblongata on the right (AAV-injected) and, to a much smaller extent, the left side of the brain (Fig. 2a). Robust staining characterized regions anatomically connected to the transduced midbrain areas that included the striatum and hypothalamus rostrally, and the locus coeruleus caudally (Fig. 2b, c) [14, 29]. This pattern of protein distribution was already observed at 2 months and persisted at 6 and 12 months post-injection.

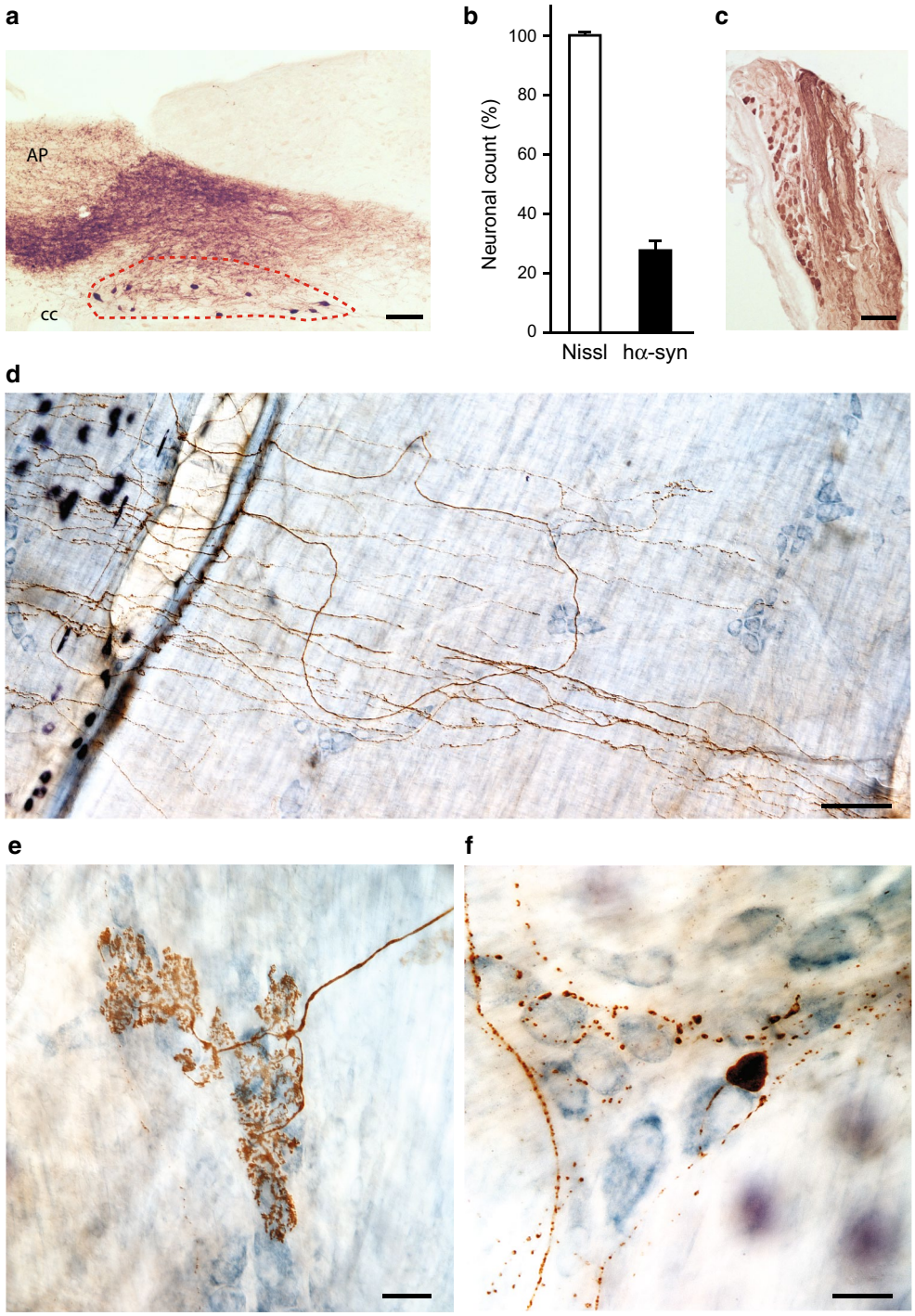

Fig. 1 Accumulation of hα-synuclein in the DMnX, nodose ganglion and gastric wall after injections of hα-synuclein-AAVs into the vagus nerve. **a**–**c** Rats ($n = 5$) received a single injection of hα-synuclein-carrying AAVs into the left vagus nerve. Analyses were performed at 2–3 weeks post-treatment. **a** A representative image shows a section of the medulla oblongata immunostained with anti-hα-synuclein; the left DMnX is delineated by *dashed lines*, and the area postrema (AP) and central canal (cc) are indicated. *Scale bar* 100 μm. **b** Medulla oblongata sections were used for stereological counting of Nissl-stained neurons (*empty bar*) and hα-synuclein-immunoreactive cells (*solid bar*) in the left DMnX. Values (mean ± SEM) are expressed as percent of the total number of Nissl-stained neurons. **c** The representative image shows neurons robustly labeled with anti-hα-synuclein in a section of the left nodose ganglion. *Scale bar* 100 μm. **d**–**f** Rats ($n = 5$) were killed 6–12 months after a single injection of hα-synuclein-carrying AAVs into the left vagus nerve. Stomach whole mounts were stained with anti-hα-synuclein and counter-stained with Cuprolinic Blue. Representative images show immunoreactive fibers and nerve terminals: long intramuscular arrays (IMAs) of rectilinear terminals (**d**), a single vagal afferent terminating as highly arborizing intraganglionic laminar endings (IGLEs) (**e**), and varicosity-rich fibers with morphological features of preganglionic vagal efferents (**f**). *Scale bars* 100 μm in **d**, 25 μm in **e** and 20 μm in **f**

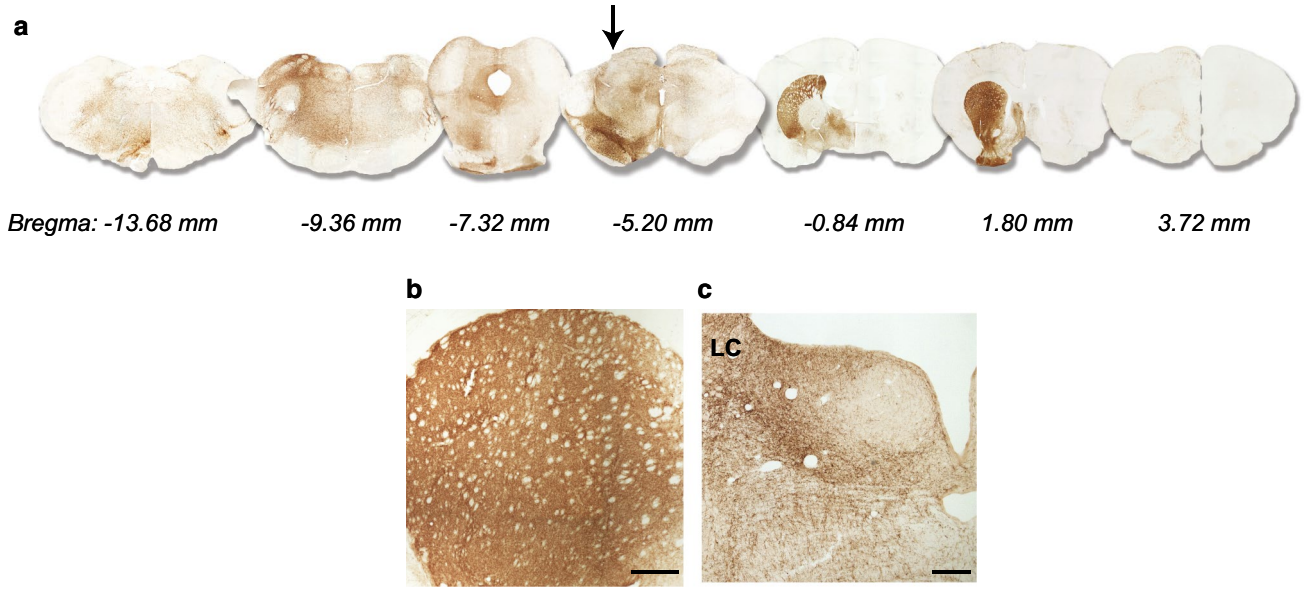

Fig. 2 Widespread brain distribution of hα-synuclein after midbrain AAV injections. Rats received a single intraparenchymal injection of hα-synuclein-AAVs into the right midbrain. **a** Analyses were made in 6 rats killed at 2 months. Representative images show brain sections at different Bregma levels stained with anti-hα-synuclein. A midbrain section containing the substantia nigra is at Bregma −5.20 mm (*arrow*). For illustration purposes, different scale factors were used to resize each section. **b**, **c** Rats ($n \geq 5$/time point) were killed at 2, 6 and 12 months post-treatment. Sections of the forebrain and pons containing the striatum (**b**) and locus coeruleus (LC) (**c**), respectively, were stained with anti-hα-synuclein. Representative images are from an animal killed at 2 months. *Scale bars* 250 μm

Stomach whole mounts of these AAV-injected rats were then assessed for immunohistochemical evidence of the exogenous protein. No immunoreactivity for hα-synuclein was observed in 6 rats killed at 2 months post-AAV injection; in contrast, hα-synuclein-positive axons and terminal varicosities were detected in the myenteric plexus of 5 out of 6 rats and 6 out of 10 animals killed at 6 and 12 months, respectively. Analysis of labeled tissues revealed the presence of markedly swollen axons (Fig. 3a). Clusters of nerve endings containing hα-synuclein encircled individual neurons (Fig. 3b, c, f) or small groups of neurons (Fig. 3d, e) within the ganglia of the plexus. The morphology and distribution of these varicosity-rich fibers were strikingly similar to previous descriptions of anterogradely labeled vagal motor nerve endings immunoreactive for endogenous α-synuclein [16, 27]. Consistent with progressive protein transfer and accumulation, myenteric ganglia with the highest density of robustly labeled terminals were found at the 12-month survival time (Fig. 3d–f). Of note, careful examination of gastric specimens for the presence of hα-synuclein-immunoreactive vagal afferents and viscerosensory terminals yielded negative results at both early and later time points post-AAV injections.

Human α-synuclein reaches nerve terminals in the stomach traveling via the vagus nerve

Accumulation of hα-synuclein within preganglionic vagal terminals of the myenteric plexus strongly suggests that, following its midbrain expression, the exogenous protein may reach peripheral tissues using the vagus nerve as a conduit. To substantiate this conclusion, a portion of the right (ipsilateral to the AAV injections) vagus nerve was collected from the neck of rats killed at 2, 6 and 12 months post-treatment. Examination of longitudinal sections of the Xth nerve stained for hα-synuclein revealed the presence of labeled fibers. Immunoreactive vagal projections were relatively rare and, for this reason, might have remained undetected even after careful evaluation of serial tissue sections. With this caveat in mind, results of our analysis indicated that hα-synuclein was absent in the vagus nerve of rats killed at 2 months ($n = 6$); labeled fibers were instead detected in >50% of nerves collected at either 6 ($n = 6$) or 12 ($n = 7$) months post-treatment (Fig. 4).

Detection of human α-synuclein protein within DMnX neurons in the medulla oblongata

Preganglionic terminals in the stomach wall originate in the DMnX, underscoring the importance that this medullary nucleus may have as a relay center for α-synuclein central-to-peripheral transmission. Experiments were therefore carried out to examine DMnX-containing medullary tissue for the presence of hα-synuclein mRNA and/or protein. Using RT-PCR, amplification reactions with hα-synuclein-hybridizing primers yielded no specific band at 3 weeks nor at 2, 6 and 12 months post-AAV treatment (Fig. 5a shows

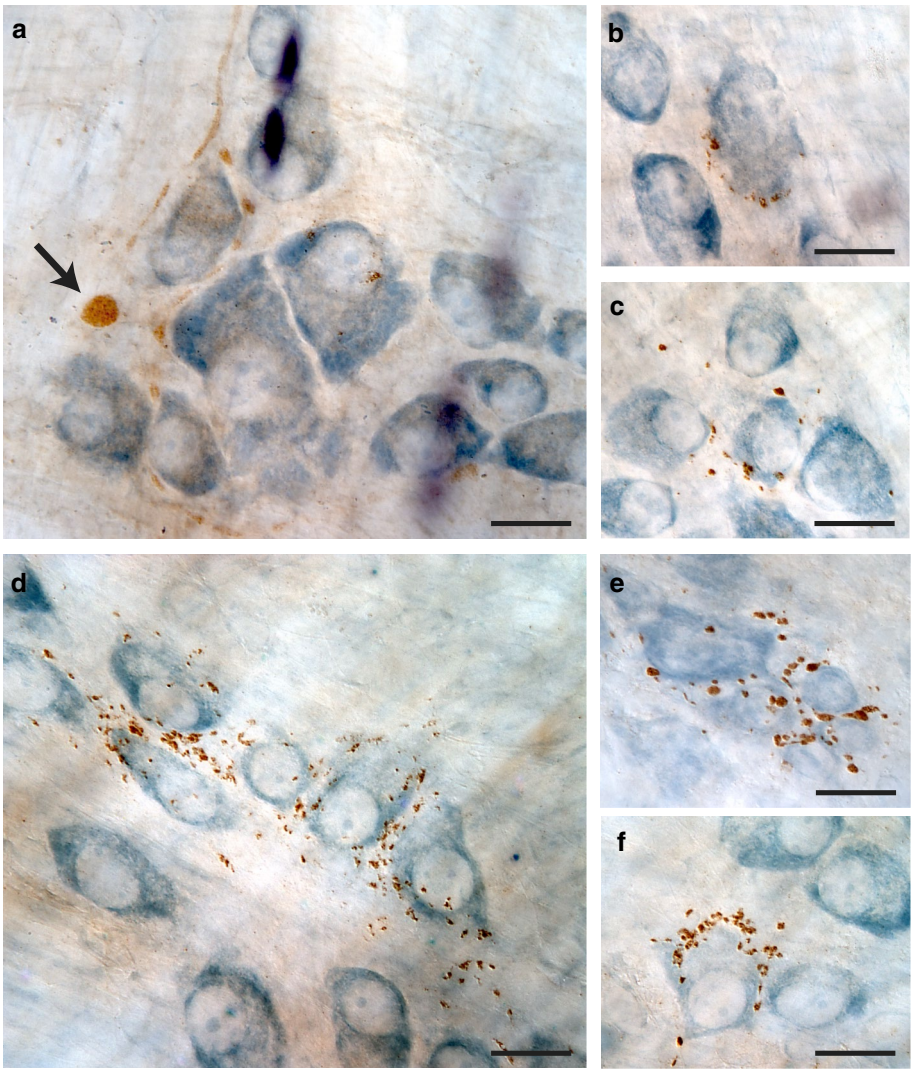

Fig. 3 Human α-synuclein immunoreactivity in the gastric wall after midbrain AAV injections. Rats received a single intraparenchymal injection of hα-synuclein-AAVs into the right midbrain. Stomach whole mounts from animals killed at 6 (**a**–**c**, $n = 6$) or 12 (**d**–**f**, $n = 10$) months post-treatment were stained with anti-hα-synuclein and counterstained with Cuprolinic Blue. Images from 5 of these animals (3 at 6 and 2 at 12 months) show a labeled swollen axon (*arrow* in **a**) and immunoreactive nerve endings around ganglionic cells (**b, c, f**) or groups of cells (**d**, **e**) of the myenteric plexus. *Scale bars* 20 μm

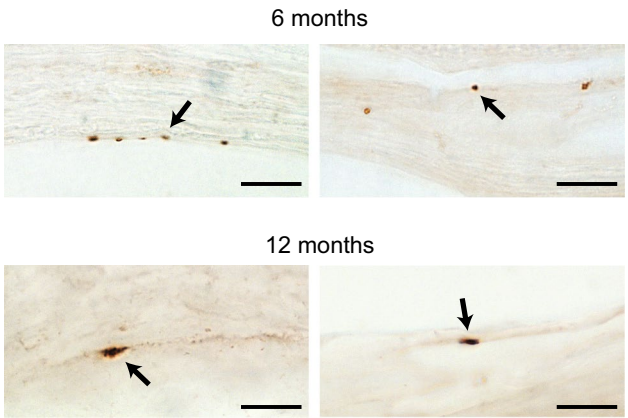

Fig. 4 Fibers of the vagus nerve containing hα-synuclein. Longitudinal sections of right vagus nerves collected from the rat neck at 6 ($n = 6$) or 12 ($n = 7$) months post-AAV-injection were stained with anti-hα-synuclein. Images from 4 of these animals, 2 at 6 and 2 at 12 months, show labeled portions of vagal fibers (*arrows*). *Scale bars* 10 μm

data at the 2-month time point). Samples were also analyzed for evidence of other AAV-derived products and, in particular, WPRE (an enhancer element incorporated into the AAV genome) mRNA. RT-PCR measurements showed lack of WPRE expression in specimens from the dorsal medulla oblongata (Fig. 5a). Similarly, WPRE mRNA was not detectable within cholinergic DMnX neurons using a highly sensitive fluorescent in situ hybridization technique coupled with immunohistochemistry [19]. Medullary tissue sections were probed with multiple WPRE-targeting oligonucleotides, yet no hybridization signal was present at either early or later time points (images at 2 months are shown in Fig. 5b, c). In situ hybridization was also carried out on tissue sections from the higher (Bregma −4.92 and −5.64 mm) and lower (Bregma −8.16 mm) midbrain and from the pons (Bregma −9.00 mm). In high-midbrain sections, neuronal cell bodies containing WPRE mRNA occupied the entire substantia nigra pars compacta (Fig. 5d), and transduced neurons were also scattered within areas

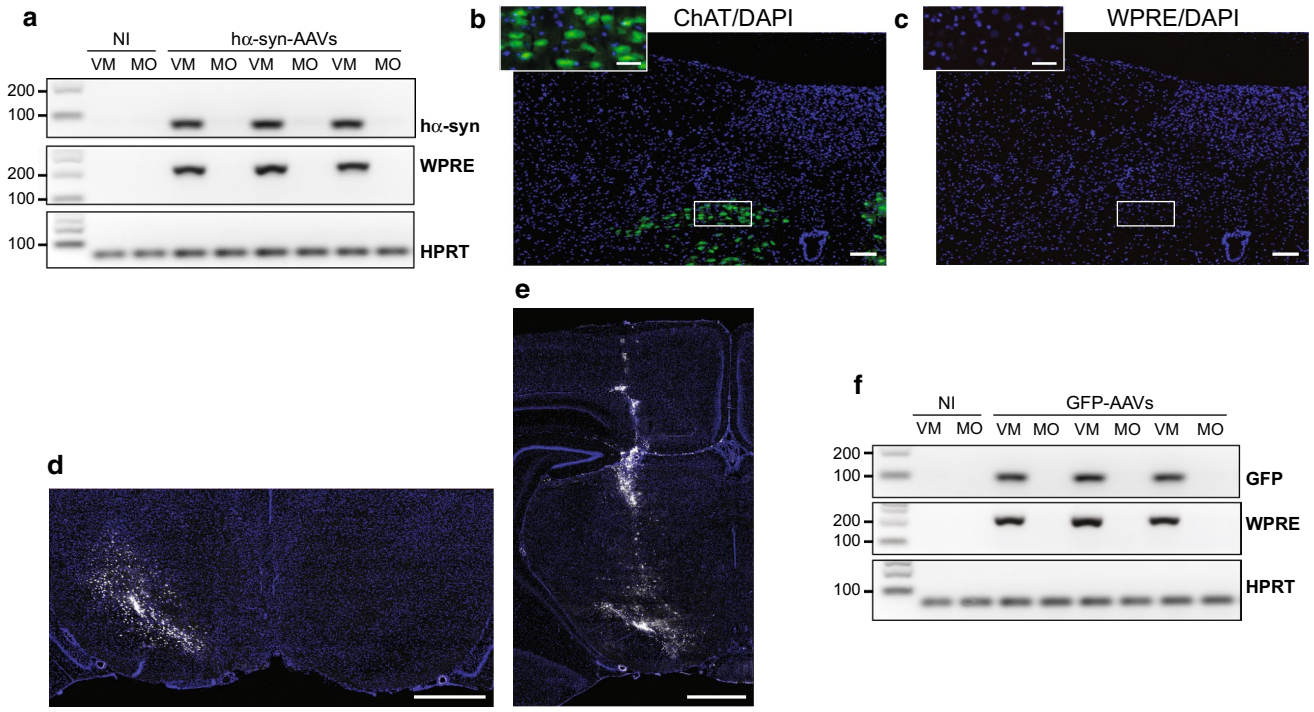

Fig. 5 Markers of transduction in the medulla oblongata and midbrain of AAV-injected rats. **a** Rats ($n = 6$) received midbrain injections of hα-synuclein-AAVs and were killed after 2 months. Non-injected (NI) animals provided control samples. Hα-synuclein (hα-syn), WPRE or hypoxanthine phosphoribosyltransferase 1 (HPRT) mRNA was assayed by RT-PCR in samples of the right (AAV-injected) ventral mesencephalon (VM) or dorso-medial medulla oblongata (MO). Specific bands were at 79 (hα-syn), 204 (WPRE), and 61 (HPRT) bp. **b, c** Medulla oblongata sections from rats injected with hα-synuclein-AAVs and killed at 2 months ($n = 4$) were processed for fluorescent in situ hybridization coupled with immunofluorescence to detect WPRE mRNA (*white*), ChAT (*green*) and DAPI (*blue*). Representative images show ChAT-positive cells (**b**) in the absence (no white signal) of WPRE hybridization (**c**). *Insets* show higher magnification images of the right DMnX. *Scale bars* 100 μm (*large panels*) and 50 μm (*insets*). **d, e** mRNA expression of WPRE (*white*) was evaluated in 4 rats killed 3 weeks after a single midbrain AAV injection. Midbrain sections were processed for fluorescent in situ hybridization and DAPI (*blue*). Representative images show right (AAV-injected) and left hemispheres (**d** Bregma = −5.64 mm) or only the right hemisphere (**e** Bregma = −4.92 mm). *Scale bars* 1 mm. **f** Rats ($n = 5$) received midbrain injections of GFP-AAVs and were killed after 2 months. Non-injected (NI) animals provided control samples. GFP, WPRE, or hypoxanthine phosphoribosyltransferase 1 (HPRT) mRNA was assayed by RT-PCR in samples of the right ventral mesencephalon (VM) or dorso-medial medulla oblongata (MO). Specific bands were at 94 (GFP), 204 (WPRE), and 61 (HPRT) bp

near the AAV injection site and needle track (Fig. 5e). No hybridization signal was instead detected in low-midbrain and pontine sections, further indicating lack of transmission/diffusion of viral particles toward brain regions distant to the mesencephalic target of AAV injections (Supplementary Figure 2).

Despite the absence of hα-synuclein mRNA and markers of AAV transduction in the lower brainstem, immunoreactivity for the exogenous protein was detected in the medulla oblongata and the DMnX; progressive burden was indicated by a time-dependent increase in axons loaded with hα-synuclein at 2, 6 and 12 months (Fig. 6a, b). Sections of the medulla oblongata containing the DMnX were also double-stained for ChAT and hα-synuclein (Fig. 6c–f). The presence of co-labeled DMnX projections supported accumulation of hα-synuclein within cholinergic vagal efferents (Fig. 6e; Supplementary Figure 3). Other DMnX axons were immunoreactive for hα-synuclein but not ChAT and likely represented neuronal projections passing through or reaching the DMnX from higher brain regions (Fig. 6f; Supplementary Figure 3). In caudal section of the medulla oblongata (e.g., Bregma –14.04 mm), ChAT-positive axons crossed the reticular formation and converged ventrolaterally to form the vagus nerve (Fig. 7a, b). Interestingly, at 6 and 12 but not 2 months post-AAV injection, a few of these intramedullary vagal fibers showed co-immunoreactivity for hα-synuclein (Fig. 7a, b).

Medullary tissue from AAV-injected rats was also stained with two conformation-specific antibodies, one that reacts with mature α-synuclein fibrils (Syn-F1) and the other recognizing both late (fibrils) and earlier (oligomers) forms of aggregated α-synuclein (Syn-O2) [12, 26]. Co-staining with Syn-F1 and ChAT very rarely identified Syn-F1-immunoreactive punctae within cholinergic vagal

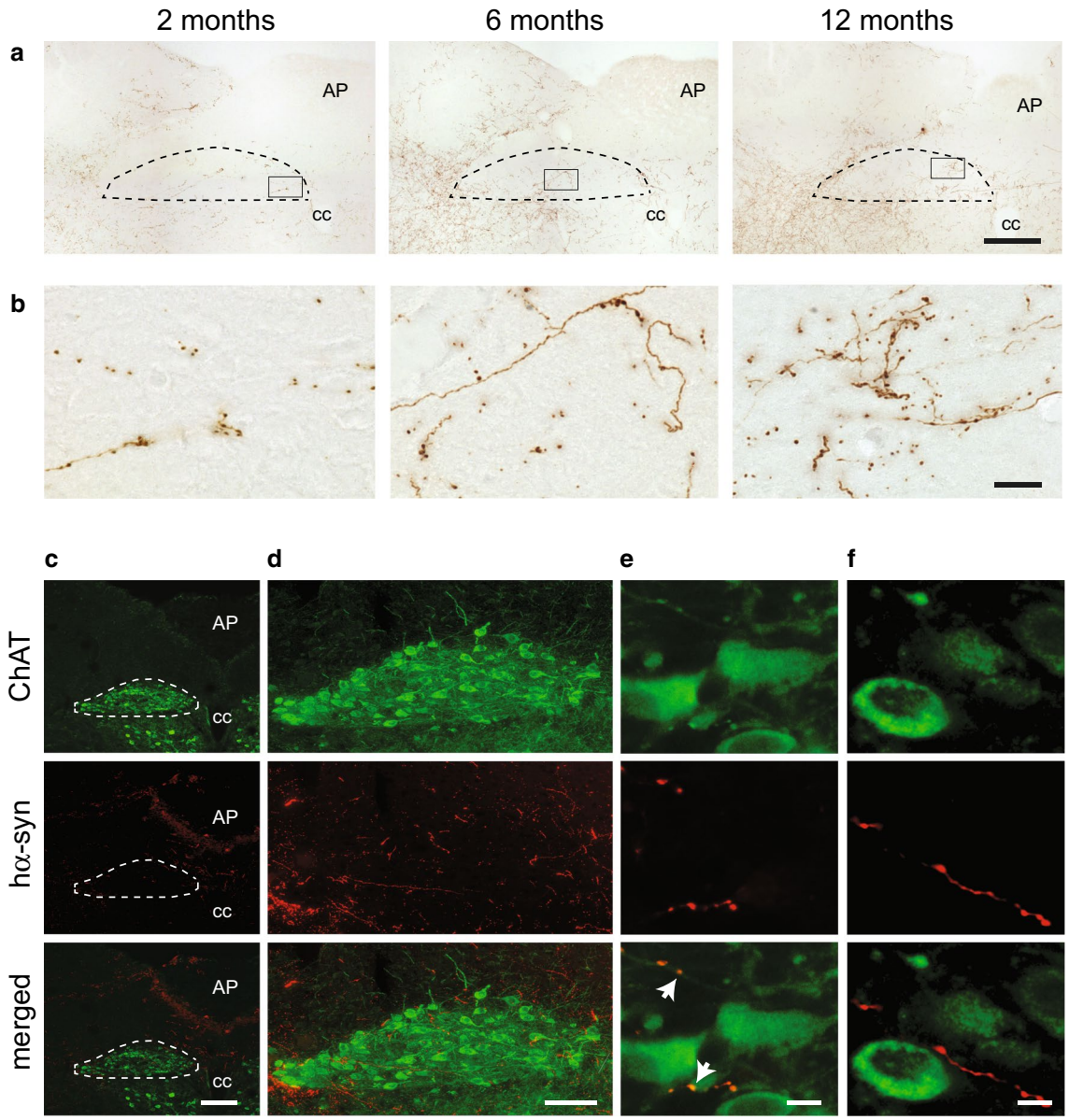

Fig. 6 Human α-synuclein protein in the DMnX of AAV-injected rats. **a**, **b** Medulla oblongata sections from rats injected with hα-synuclein-AAVs ($n \geq 5$/time point) were immunostained with anti-hα-synuclein. Representative images at lower magnification (**a**) show labeled neuronal projections in the right medulla oblongata; the DMnX is delineated by *dashed lines*, and the area postrema (AP) and central canal (cc) are indicated. *Rectangular boxes* encompass portions of the right DMnX that are also shown at higher magnification (**b**). *Scale bars* 200 μm in **a** and 20 μm in **b**. **c**–**f** Rats ($n = 5$) received a single midbrain injection of hα-synuclein-AAVs and were killed 6 months later. Sections of the medulla oblongata were double-stained with anti-ChAT and anti-hα-synuclein (hα-syn). The right DMnX is delineated by *dashed lines* at low magnification (**c**) and shown in its entireness in **d**. Images at high magnification (**e**, **f**) show DMnX axons co-labeled with hα-syn and ChAT (**e** *white arrows* in the merged panel), or immunoreactive for hα-syn but not ChAT (**f**). *Scale bars* 200 μm in **c**, 100 μm in **d** and 10 μm in **e**, **f**

projections even at later time points (Fig. 7c). Syn-O2 immunoreactivity was more robust and readily detectable in all AAV-injected rats. As shown in Fig. 7d, entire profiles of intramedullary vagal fibers could be distinguished by Syn-O2/ChAT co-labeling. For comparative purposes, tissue sections from the high-midbrain were also stained with Syn-F1 or Syn-O2; with either of the two antibodies, intense and diffuse immunoreactivity was observed within and outside the substantia nigra, labeling both neuronal cell bodies and neuronal projections of AAV-injected rats (Supplementary Figure 4).

A final set of experiments was carried out in rats that received unilateral midbrain injections of GFP- rather than hα-synuclein-carrying AAVs. GFP-AAV administration

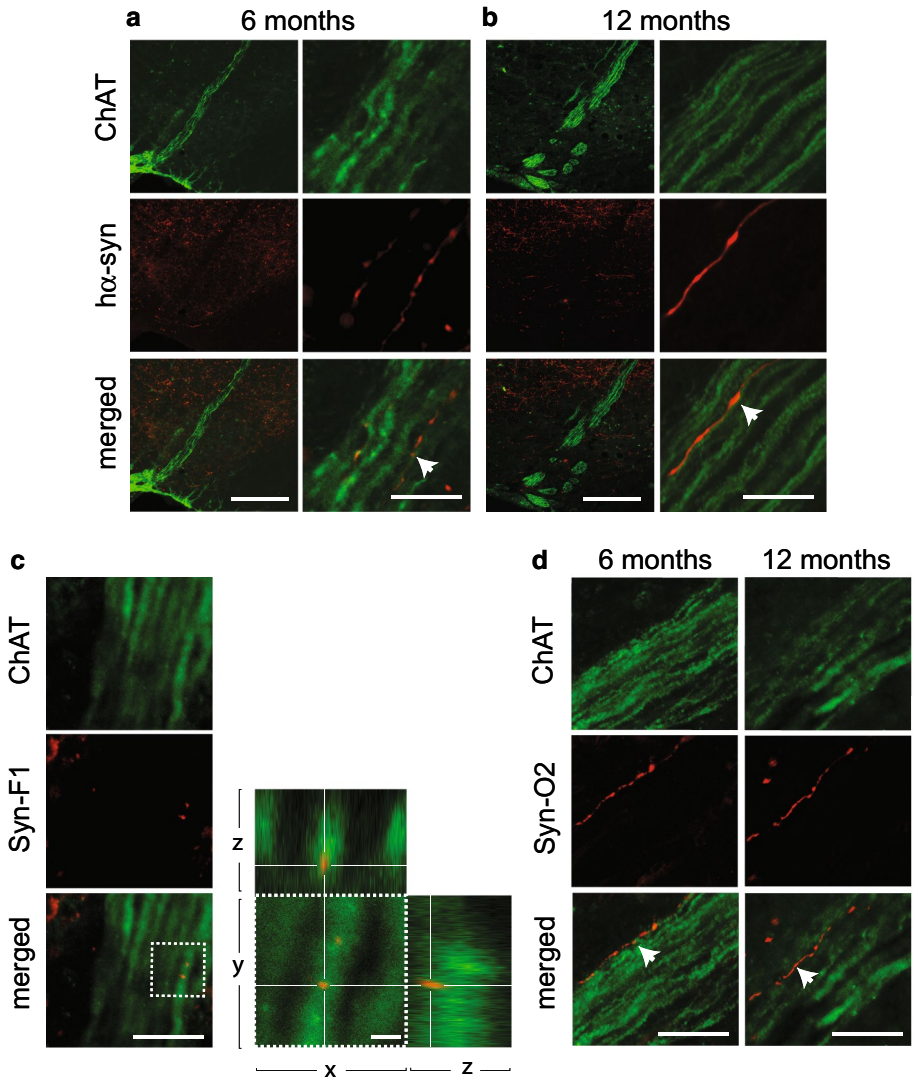

Fig. 7 Human α-synuclein-positive vagal axons in the rat medulla oblongata. **a**, **b** Rats ($n = 5$/time point) received a single midbrain injection of hα-synuclein-AAVs. Sections of the lower medulla oblongata (between Bregma −13.92 and −14.04 mm) were double-stained with anti-ChAT and anti-hα-synuclein. Images at lower magnification (*left panels*) show bundles of fibers that cross the right medulla oblongata converging into the vagus nerve. Higher magnification panels (*right*) show intramedullary vagal fibers co-labeled for ChAT and hα-synuclein (some of these fibers are indicated by *white arrows*). *Scale bars* 200 μm (*lower magnification*) and 10 μm (*higher magnification*). **c** Rats ($n = 5$) were killed at 12 months after a single midbrain injection of hα-synuclein-AAVs. Sections of the lower medulla oblongata were double-stained with anti-ChAT plus an antibody that specifically recognizes mature α-synuclein fibrils (Syn-F1). Images show co-labeled punctae within a vagal axon crossing the reticular formation of the right medulla oblongata. Co-localization was confirmed in the enlarged images showing orthogonal cross-sections in the *x*–*y*, *x*–*z* and *y*–*z* axes. *Scale bars* 10 μm (*lower magnification*) and 2 μm (*higher magnification*). **d** Rats ($n = 5$/time point) were killed at 6 and 12 months after a single midbrain injection of hα-synuclein-AAVs. Sections of the lower medulla oblongata were double-stained with anti-ChAT plus an antibody that recognizes oligomeric and fibrillar forms of α-synuclein (Syn-O2). Images show co-labeled vagal axons (*white arrows* in the merged panels) in the right medulla oblongata. *Scale bar* 10 μm

caused transduction features similar to those observed with hα-synuclein-AAVs; robust transduction was measured in midbrain samples, whereas WPRE mRNA remained undetectable in specimens from the dorsal medulla oblongata (Fig. 5f). In contrast to the results with hα-synuclein-AAVs, however, GFP-AAV injections were not associated with presence of the transduced protein in vagal neurons; no GFP immunoreactivity was indeed observed within DMnX cholinergic axons in the medulla oblongata (Supplementary Figure 5a). Similarly, vagus nerve sections and stomach whole mount preparations were consistently devoid of GFP labeling (Supplementary Figure 5b, c).

Discussion

Results of this study reveal a distinctive role of DMnX-derived vagal efferents in transferring α-synuclein from the brain to peripheral tissues. When hα-synuclein was overexpressed directly in the vagal system (DMnX and vagal ganglia), it efficiently traveled via both efferent and afferent fibers of the vagus nerve and reached visceromotor as well as viscerosensory terminals in the stomach wall (Fig. 8a). Quite in contrast, protein overexpression targeted to the midbrain resulted in detection and accumulation of hα-synuclein only within vagal efferents terminating onto ganglionic neurons of the myenteric plexus (Fig. 8b). This preferential route of protein transmission is particularly remarkable if one considers that preganglionic efferents represent only a small percent of fibers forming the vagus nerve and that, based on their numerical prevalence within this nerve, a greater contribution of sensory afferents to α-synuclein transfer might have been expected. Indeed, according to estimates in various animal species and with different techniques, the ratio of efferent over afferent vagal projections has been reported to range between 1:10 and 1:3 [1, 18]. Our present study focused on α-synuclein transmission from the brain to the gastric wall. However, given the extensive innervation provided to the small intestine by vagal preganglionic efferents [4], it is conceivable that α-synuclein may also travel from the brain to other sections of the gastrointestinal tract, such as the duodenum and jejunum. Further work is warranted to substantiate this possibility and determine whether accumulation of brain-derived α-synuclein throughout the gut may result in overt alterations of gastrointestinal function in this animal model.

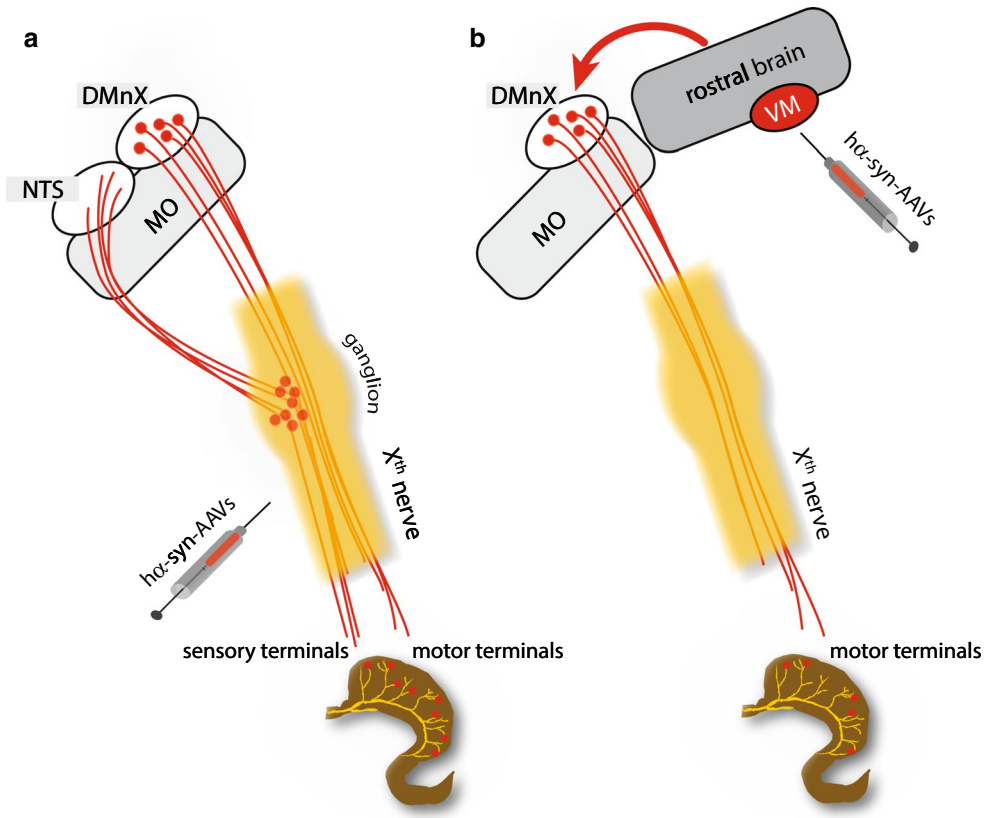

Fig. 8 Schematic representations of patterns of hα-synuclein accumulation after vagal or intraparenchymal injections of hα-synuclein-AAVs. **a** Following AAV injections into the vagus nerve, neuronal cell bodies in the DMnX and nodose ganglion produce hα-synuclein. The exogenous protein is then accumulated within efferent DMnX projections and afferent vagal fibers, reaching both visceromotor and viscerosensory nerve endings in the gastric wall. Afferent fibers also terminate onto neurons of the nucleus of the tractus solitarius (NTS) in the medulla oblongata (MO). **b** Following AAV injections into the ventral mesencephalon (VM), hα-synuclein is overexpressed within neurons that project toward lower brainstem regions. Traveling rostro-caudally through these axons, the exogenous protein reaches the medulla oblongata (MO) and gains access into DMnX neurons. The red arrow underscores the fact that passage into these cells would require a neuron-to-neuron jump. Hα-synuclein then uses efferent projections stemming from the DMnX and contained in the vagus nerve to reach preganglionic vagal nerve endings in the stomach wall

Specific mechanisms underlying the propensity of visceromotor vagal fibers to accrue and deliver α-synuclein remain unclear. Braak and colleagues underscored a potential relationship between axonal length and myelination and vulnerability to α-synuclein pathology; morphological and metabolic differences between long, thin and poorly myelinated axons of the visceromotor vagal system vs. sturdily myelinated fibers relaying viscerosensory inputs may contribute to their distinctive role in pathological processes involving α-synuclein [6]. It is also noteworthy that earlier work investigating endogenous α-synuclein expression in the rat stomach and duodenum found that vagal afferent endings did not contain α-synuclein, whereas virtually all vagal preganglionic projections expressed the protein [16]. It appears therefore that vagal neurons producing, transporting and utilizing α-synuclein under normal conditions may more efficiently serve as conduits for pathological protein transfer and be more vulnerable to α-synuclein accumulation.

Hα-synuclein was detected within cholinergic DMnX axons (by 2 months), within intramedullary fibers of the Xth nerve and within the vagus nerve itself in the rat neck (by 6 months), supporting the conclusion that brain-to-stomach protein advancement progressively occurred through this pathway (Fig. 8b). The DMnX encompasses cholinergic cell bodies that only project outside the brain via axons forming the Xth cranial nerve (Fig. 8b). Data are therefore consistent with the interpretation that hα-synuclein, once generated within transduced midbrain neurons, proceeded toward the medulla oblongata and gained access into DMnX cells as a result of both intra- and inter-neuronal protein transfer. Based on our findings with conformation-specific antibodies, monomeric and oligomeric forms of α-synuclein are likely to be primarily responsible for protein mobility. Crowding of α-synuclein within vagal neurons may subsequently trigger a localized process of further aggregation, leading to the formation of mature α-synuclein fibrils. An alternative explanation for the vagal accumulation of exogenous α-synuclein under our experimental conditions might have been that viral vectors injected into the ventral mesencephalon were able to reach and transduce DMnX cells. Several lines of evidence make this possibility highly unlikely. They include lack of detection of hα-synuclein mRNA and lack of hybridization of multiple oligonucleotides targeting WPRE mRNA (a viral vector marker) in DMnX-containing medullary tissue. Furthermore, midbrain injections of GFP-carrying AAVs did not result in any detection of GFP protein within DMnX neurons, underscoring the inability of these viral vectors to travel to the medulla oblongata and transduce vagal cells. Finally, a relatively non-specific diffusion of hα-synuclein-carrying AAVs would be difficult to reconcile with our observation of a targeted protein accumulation within preganglionic vagal efferents.

Together with earlier observations supporting a gut-to-brain transfer of α-synuclein [13, 15], our current findings indicate that protein transmission can proceed in either direction from distant organs to the brain or from the brain to peripheral tissues. This bidirectional potential is consistent with the ability of α-synuclein to move both anterogradely and retrogradely within neurons [7–9, 23]. An important translational implication of our study concerns the presence of α-synuclein pathology in peripheral tissues of synucleinopathy patients. Pathological forms of the protein have been detected in the gastrointestinal tract of patients with Parkinson's disease as well as multiple system atrophy and dementia with Lewy bodies [3, 17, 20]. In some instances, these peripheral α-synuclein lesions were observed in non-symptomatic individuals, suggesting that they may represent initial or early manifestations of Parkinson's disease [5, 21]. Our current results do not confute this possibility. They clearly indicate, however, that accumulation of α-synuclein in peripheral tissues may not always define site(s) of disease inception or be a marker of prodromal disease stages. The pattern of progression of α-synuclein pathology, caudo-rostral or rostro-caudal, may vary from patient to patient and differ, for example, in typical Parkinson's disease as compared to sub-variants of the disease or other synucleinopathies.

Acknowledgements We thank Sarah A. Jewell for her comments on the manuscript, Omar El-Agnaf for kindly providing conformation-specific antibodies, Raffaella Rusconi for the design of in situ probes, Cherie N. Hudson, Bettina Winzen-Reichert, Franziska Hesse, Laura Jakobi for assistance with the experiments, and Ireen Koenig for assistance with microscopy. This work was supported by the Paul Foundation, the Centres of Excellence in Neurodegeneration Research (CoEN) and NIH Grant DK027627.

References

1. Agostoni E, Chinnock JE, De Daly MB, Murray JG (1957) Functional and histological studies of the vagus nerve and its branches to the heart, lungs and abdominal viscera in the cat. J Physiol 135:182–205
2. Annerino DM, Arshad S, Taylor GM, Adler CH, Beach TG, Greene JG (2012) Parkinson's disease is not associated with gastrointestinal myenteric ganglion neuron loss. Acta Neuropathol 124:665–680. doi:10.1007/s00401-012-1040-2
3. Beach TG, Adler CH, Sue LI, Vedders L, Lue L, White Iii CL, Akiyama H, Caviness JN, Shill HA, Sabbagh MN, Walker DG (2010) Multi-organ distribution of phosphorylated α-synuclein histopathology in subjects with Lewy body disorders. Acta Neuropathol 119:689–702. doi:10.1007/s00401-010-0664-3
4. Berthoud HR, Jedrzejewska A, Powley TL (1990) Simultaneous labeling of vagal innervation of the gut and afferent projections from the visceral forebrain with dil injected into the dorsal vagal complex in the rat. J Comp Neurol 301:65–79

5. Braak H, de Vos RA, Bohl J, Del Tredici K (2006) Gastric α-synuclein immunoreactive inclusions in Meissner's and Auerbach's plexuses in cases staged for Parkinson's disease-related brain pathology. Neurosci Lett 396:67–72. doi:10.1016/j.neulet.2005.11.012
6. Braak H, Rub U, Gai WP, Del Tredici K (2003) Idiopathic Parkinson's disease: possible routes by which vulnerable neuronal types may be subject to neuroinvasion by an unknown pathogen. J Neural Transm 110:517–536. doi:10.1007/s00702-002-0808-2
7. Danzer KM, Kranich LR, Ruf WP, Cagsal-Getkin O, Winslow AR, Zhu L, Vanderburg CR, McLean PJ (2012) Exosomal cell-to-cell transmission of α-synuclein oligomers. Mol Neurodegener 7:42. doi:10.1186/1750-1326-7-42
8. Freundt EC, Maynard N, Clancy EK, Roy S, Bousset L, Sourigues Y, Covert M, Melki R, Kirkegaard K, Brahic M (2012) Neuron-to-neuron transmission of α-synuclein fibrils through axonal transport. Ann Neurol 72:517–524. doi:10.1002/ana.23747
9. George S, Rey NL, Reichenbach N, Steiner JA, Brundin P (2013) α-Synuclein: the long distance runner. Brain Pathol 23:350–357. doi:10.1111/bpa.12046
10. Giasson BI, Jakes R, Goedert M, Duda JE, Leight S, Trojanowski JQ, Lee VM (2000) A panel of epitope-specific antibodies detects protein domains distributed throughout human α-synuclein in Lewy bodies of Parkinson's disease. J Neurosci Res 59:528–533
11. Goedert M, Spillantini MG, Del Tredici K, Braak H (2013) 100 years of Lewy pathology. Nat Rev Neurol 9:13–24. doi:10.1038/nrneurol.2012.242
12. Helwig M, Klinkenberg M, Rusconi R, Musgrove RE, Majbour NK, El-Agnaf OM, Ulusoy A, Di Monte DA (2016) Brain propagation of transduced α-synuclein involves non-fibrillar protein species and is enhanced in α-synuclein null mice. Brain 139:856–870. doi:10.1093/brain/awv376
13. Holmqvist S, Chutna O, Bousset L, Aldrin-Kirk P, Li W, Bjorklund T, Wang ZY, Roybon L, Melki R, Li JY (2014) Direct evidence of Parkinson pathology spread from the gastrointestinal tract to the brain in rats. Acta Neuropathol 128:805–820. doi:10.1007/s00401-014-1343-6
14. Kirik D, Rosenblad C, Burger C, Lundberg C, Johansen TE, Muzyczka N, Mandel RJ, Bjorklund A (2002) Parkinson-like neurodegeneration induced by targeted overexpression of α-synuclein in the nigrostriatal system. J Neurosci 22:2780–2791
15. Pan-Montojo F, Schwarz M, Winkler C, Arnhold M, O'Sullivan GA, Pal A et al (2012) Environmental toxins trigger PD-like progression via increased α-synuclein release from enteric neurons in mice. Sci Rep 2:898. doi:10.1038/srep00898
16. Phillips RJ, Walter GC, Wilder SL, Baronowsky EA, Powley TL (2008) α-Synuclein-immunopositive myenteric neurons and vagal preganglionic terminals: autonomic pathway implicated in Parkinson's disease? Neuroscience 153:733–750. doi:10.1016/j.neuroscience.2008.02.074
17. Pouclet H, Lebouvier T, Coron E, Rouaud T, Flamant M, Toulgoat F, Roy M, Vavasseur F, Bruley des Varannes S, Neunlist M, Derkinderen P (2012) Analysis of colonic α-synuclein pathology in multiple system atrophy. Parkinsonism Relat Disord 18:893–895. doi:10.1016/j.parkreldis.2012.04.020
18. Prechtl JC, Powley TL (1990) The fiber composition of the abdominal vagus of the rat. Anat Embryol 181:101–115
19. Raj A, van den Bogaard P, Rifkin SA, van Oudenaarden A, Tyagi S (2008) Imaging individual mRNA molecules using multiple singly labeled probes. Nat Methods 5:877–879. doi:10.1038/nmeth.1253
20. Sánchez-Ferro Á, Rábano A, Catalán MJ, Rodríguez-Valcárcel FC, Fernández Díez S, Herreros-Rodríguez J, Garcia-Cobos E, Alvarez-Santullano MM, Lopez-Manzanares L, Mosqueira AJ, Vela Desojo L, Lopez-Lozano JJ, Lopez-Valdes E, Sanchez-Sanchez R, Molina-Arjona JA (2015) In vivo gastric detection of α-synuclein inclusions in Parkinson's disease. Mov Disord 30:517–524. doi:10.1002/mds.25988
21. Shannon KM, Keshavarzian A, Dodiya HB, Jakate S, Kordower JH (2012) Is α-synuclein in the colon a biomarker for premotor Parkinson's disease? Evidence from 3 cases. Mov Disord 27:716–719. doi:10.1002/mds.25020
22. Spillantini MG, Schmidt ML, Lee VM, Trojanowski JQ, Jakes R, Goedert M (1997) α-Synuclein in Lewy bodies. Nature 388:839–840. doi:10.1038/42166
23. Uchihara T, Giasson B (2016) Propagation of α-synuclein pathology: hypotheses, discoveries, and yet unresolved questions from experimental and human brain studies. Acta Neuropathol 131:49–73. doi:10.1007/s00401-015-1485-1
24. Ulusoy A, Musgrove RE, Rusconi R, Klinkenberg M, Helwig M, Schneider A, Di Monte DA (2015) Neuron-to-neuron α-synuclein propagation in vivo is independent of neuronal injury. Acta Neuropathol Commun 3:13. doi:10.1186/s40478-015-0198-y
25. Ulusoy A, Rusconi R, Perez-Revuelta BI, Musgrove RE, Helwig M, Winzen-Reichert B, Di Monte DA (2013) Caudo-rostral brain spreading of α-synuclein through vagal connections. EMBO Mol Med 5:1051–1059. doi:10.1002/emmm.201302475
26. Vaikath NN, Majbour NK, Paleologou KE, Ardah MT, van Dam E, van de Berg WD, Forrest SL, Parkkinen L, Gai WP, Hattori N, Takanashi M, Lee SJ, Mann DM, Imai Y, Halliday GM, Li JY, El-Agnaf OM (2015) Generation and characterization of novel conformation-specific monoclonal antibodies for α-synuclein pathology. Neurobiol Dis 79:81–99. doi:10.1016/j.nbd.2015.04.009
27. Walter GC, Phillips RJ, Baronowsky EA, Powley TL (2009) Versatile, high-resolution anterograde labeling of vagal efferent projections with dextran amines. J Neurosci Methods 178:1–9. doi:10.1016/j.jneumeth.2008.11.003
28. Wang FB, Powley TL (2000) Topographic inventories of vagal afferents in gastrointestinal muscle. J Comp Neurol 421:302–324
29. Wang ZY, Lian H, Cai QQ, Song HY, Zhang XL, Zhou L, Zhang YM, Zheng LF, Zhu JX (2014) No direct projection is observed from the substantia nigra to the dorsal vagus complex in the rat. J Parkinsons Dis 4:375–383. doi:10.3233/JPD-130279